Chemistry and microstructure of orthoamphiboles from cordierite–amphibole rocks at Outokumpu, North Karelia, Finland

Peter J. Treloar and Andrew Putnis

Department of Earth Sciences, University of Cambridge, Cambridge CB2 3EQ

ABSTRACT. Orthoamphiboles from the cordierite–amphibole-bearing rocks at Outokumpu span a large part of the gedrite–anthophyllite solid-solution series. The amphiboles grew at temperatures near to or just above that of the solvus crest with post-metamorphic cooling resulting in sub-solvus exsolution, the distribution of which is compatible with an asymmetric solvus in which the anthophyllite limb is the steeper. Metamorphic conditions in the area imply that the crest of the solvus is unlikely to be at a temperature in excess of about 600 °C. Electron microprobe traverses and Al-$K\alpha$ scans show that the amphibole compositions vary rapidly both along and across grains. These variations can be explained by varying availability of Na controlling the extent of the edenitic substitution in the solid solution series. In this case this variability in Na availability may be explained by the external control of μ_{Na} through the fluid phase.

THE existence of a solvus in the orthoamphibole solid-solution series between anthophyllite and gedrite has been demonstrated by a number of workers, notably Robinson and co-workers (Robinson and Jaffe, 1969; Robinson et al., 1971; Ross et al., 1969) and more recently by Stoddard (1979) and Spear (1980). Two major substitutions, edenitic (Na,Al $\rightleftharpoons$ $\square$Si) and tschermakitic (Al^{VI}, Al^{IV} $\rightleftharpoons$ Mg,Si), are operative in the solid-solution series between low Na–Al anthophyllite and high Na–Al gedrites with the solvus defined by gaps in the substitutions. The effect of the solvus is seen both in the simultaneous growth of equilibrium anthophyllite-rich and gedrite-rich orthoamphiboles (Spear, 1980) and in the development of exsolution lamellae during sub-solvus cooling (Gittos et al., 1976).

In the cordierite–amphibole-bearing rocks of the Outokumpu ore district in Finland rapid variations in the amount of the solid-solution substitutions are observed within individual grains. Some, but not all, of these variations may be solvus related. This paper describes the chemistry of these ortho-amphiboles with the aim of commenting on the effect of the solvus on their growth and subsequent behaviour.

Geological background. The stratiform ore deposits of the Outokumpu region of North Karelia, Finland lie within the mica schists and black schists of the Outokumpu Formation (Mikkola, 1980). A suite of rocks termed the 'Outokumpu Association' (Gaal et al., 1975) and largely comprising skarns, quartzites, carbonates, and serpentinites occur in close proximity to the ore deposits to which they appear to be genetically related. A rock type which has previously been termed 'cordierite–anthophyllite rock' (Gaal et al., 1975) forms a limited part of the Outokumpu Association and it is with this particular rock that this paper is concerned. The term cordierite–anthophyllite rock is a misnomer as these rocks contain very little pure anthophyllite, and may be best described as cordierite–amphibole-bearing rocks.

Huhma and Huhma (1970), Makela (1974), and Peltola (1978) have postulated a submarine exhalative–sedimentary origin for the Outokumpu ore deposit, associated with sea-floor serpentinization and carbonatization of basic rocks, the quartzite being a chemical colloidal precipitate formed as a part of this alteration process. The peculiar chemistry of the cordierite–amphibole-bearing rocks, which are Ca free, Si poor and Mg and Fe enriched, dates from this period, being the result of leaching by fluid movement during the submarine alteration process (cf. Vallance, 1967). Structural (Koistinen, 1981) and petrological and chemical (Treloar et al., 1981) studies support the resultant view that the mineralogy of the cordierite–amphibole-bearing rocks is the consequence of the metamorphism of a sedimentary rock of unusual chemistry, rather than the classic view that the mineralogy results from metasomatism during syn-metamorphic ore genesis (Eskola, 1933; Tuominen and Mikkola, 1950).

Conditions of metamorphism have been estimated from a consideration of the assemblages contained within both the cordierite–amphibole-bearing rocks and the regionally developed mica-schists. $P–T$ conditions of 3.5 ± 1 kb and $600 \pm 50\,°C$ are indicated (Treloar *et al.*, 1981) and these are compatible with the regional geothermal gradient inferred by Campbell (1980).

Phase petrology and chemistry. The present rocks contain a wide diversity of phases including two distinct amphiboles, an orthoamphibole and a Ca-free clinoamphibole, either garnet or staurolite, cordierite, biotite, chlorite (much of which is secondary), ilmenite, pyrrhotine, and a spinel solid-solution phase. They do not contain free quartz, aluminium silicate or corundum and thus may be considered to be significantly different from otherwise similar rocks discussed elsewhere (e.g. Robinson and Jaffe, 1969; James *et al.*, 1978). Key phases within this assemblage are the amphiboles together with the cordierite, garnet, and staurolite.

Amphiboles occur as large bladed crystals typically 1 to 6 mm in length, though occasionally several cm long. Basal sections may be up to 4 or 5 mm in diameter. The common occurrence is in sheath-like groups which define a strong metamorphic foliation which is not necessarily parallel to an original layering. Occasional radial aggregates have been developed, and in some instances an individual crystal may occur at a high angle to the dominant foliation. Both ortho- and clino-amphiboles behave in the same way, occurring next to each other in sheath-like aggregates.

Of the other major phases, staurolite occurs as prismatic crystals up to 5 mm in length and garnet as rounded crystals, always greater than 2 mm in diameter and up to, in one instance, 1.5 cm in diameter. A considerable proportion of the matrix material between the amphiboles is cordierite, which occurs as ragged porphyroblasts up to 6 mm in diameter. Between 80 and 90% of the rock is constituted solely of amphibole and cordierite, with the amphibole, mostly orthoamphibole, forming over 50% of the whole.

The composition of orthoamphiboles and their coexisting phases are shown on a plot of (Al–Na)–Fe–Mg (fig. 1). This diagram should not be regarded as a projection and is simply meant to show compositional variations within a limiting system. It includes data from nine different rocks.

Within any one rock cordierite, staurolite, and clinoamphibole are all constant in composition. Garnet shows marked zoning with $X_{mg}^{rim} > X_{mg}^{core}$. Values of K_D^{Mg-Fe} between cordierite and staurolite, clinoamphibole, orthoamphibole, garnet core, and garnet rim are constant from one rock to another. Cummingtonite normally has X_{mg} 2% greater than associated orthoamphibole.

This pattern of an association of phases all with restricted compositions and all in mutual equilibrium is disturbed by the orthoamphiboles which, while they retain a near-constant Fe : Mg ratio, show a complete range in Na and Al content of up to 0.42 formula units Na, and between 0.20 and 2.88 formula units Al, corresponding to a range in composition from $Anth_{94}Gedr_6$ to $Anth_{22}Gedr_{78}$. This forms a significant part of the anthophyllite-gedrite solid-solution series and may be observed not only in individual rocks but also in individual crystals.

In view of the apparent equilibrium behaviour of the co-existing phases these rapid variations may be unexpected. The following sections explore the chemistry of the orthoamphiboles with the aim of elucidating their behavioural history.

Orthoamphibole chemistry. Representative analyses of orthoamphiboles from the present rocks (Table I) reinforce the graphical impression of fig. 1 that there is a continuous gradation through the orthoamphibole solid solution series. All iron is listed as Fe^{2+}. A plot of tetrahedral Al *vs.* Na shows a similar continuous gradation (fig. 2). All analyses have been carried out on an EDS electron-probe and due to the high detection levels of Na
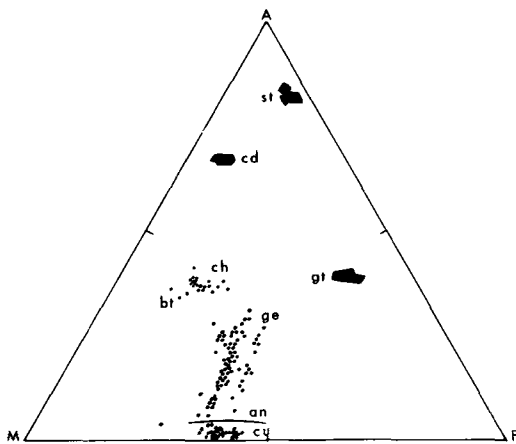

FIG. 1. A–F–M plot of phase compositions from the amphibole–cordierite-bearing rocks of Outokumpu (A = Al_2O_3–Na_2O–CaO, F = FeO + MnO, M = MgO).
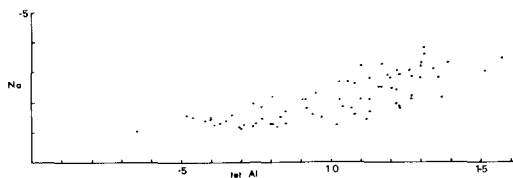

FIG. 2. Plot of Na *vs.* tetrahedral Al in orthoamphiboles.

on such a machine this plot is by necessity incomplete in that it cannot include points with a low Na content. There is a scatter about a linear trend not far removed from 4Al to 1Na, which is similar to that reported elsewhere by Robinson *et al.* (1971) and Spear (1980) and which is the effect of the edenite and tschermakite substitutions.

Spot traverses (fig. 3) and Al-$K\alpha$ scans (fig. 4) indicate that this gradation through the solid-solution series is identifiable within individual crystals. Rapid variations in crystal chemistry may be observed in all directions within an individual crystal. Some areas show a division into broad Al-rich and Al-poor bands (fig. 4a) within which there may be considerable variations (fig. 3a) while other areas may show more rapid alternations between the Al-rich and Al-poor bands. These bands, running parallel to the c-axis, do not show continuity along the grains, all of them being discontinuous, often with ragged terminations

TABLE I. Orthoamphibole compositions

SiO_2	45.25	45.19	45.69	46.72	46.71	46.34	48.23	48.06	42.96	49.41	50.31	49.82	51.00	51.04	52.36	52.14	52.27
Al_2O_3	17.21	16.02	14.87	14.20	13.42	12.86	12.41	11.86	10.39	10.05	9.26	8.70	7.51	7.26	6.88	6.00	5.35
Cr_2O_3	0.18	0.56	0.27	0.37	0.26	0.22	0.16	0.14	0.17	0.21	0.13	0.15	0.30	bd	0.13	0.12	0.13
TiO_2	0.15	0.13.	0.13	bd	bd	bd	0.14	bd	bd	bd	bd	bd	bd	0.12	bd	bd	bd
FeO	20.91	20.28	21.08	19.87	20.54	23.00	18.00	19.62	23.38	20.71	21.04	23.17	21.08	20.55	20.85	20.81	24.26
MgO	14.29	14.68	14.41	16.17	15.43	14.01	17.48	16.62	14.73	16.86	17.63	15.97	17.94	18.19	18.72	18.65	16.96
MnO	0.12	0.14	0.21	0.22	0.12	bd	0.37	0.24	bd.	0.12	0.26	bd	0.25	0.15	bd	0.15	bd
CaO	0.33	0.42	0.32	0.23	0.42	0.25	0.41	0.14	0.21	bd	0.10	0.18	0.16	0.08	bd	0.10	0.19
Na_2O	1.26	1.02	0.77	1.12	0.57	1.02	0.77	0.56	0.52	0.75	0.47	0.46	0.45	bd	0.46	bd	bd
	99.70	98.56	97.75	98.90	97.47	97.71	97.97	97.24	97.36	98.11	99.18	98.45	98.69	97.39	99.40	97.97	99.16
Si	6.43	6.49	6.63	6.67	6.77	6.77	6.87	6.93	7.03	7.09	7.15	7.20	7.29	7.35	7.39	7.47	7.51
Al	2.88	2.72	2.54	2.39	2.29	2.21	2.09	2.02	1.79	1.70	1.55	1.48	1.27	1.23	1.15	1.01	0.91
Cr	0.02	0.06	0.03	0.04	0.03	0.03	0.02	0.02	0.02	0.01	0.01	0.02	0.03		0.01	0.01	0.02
Ti	0.02	0.01	0.01				0.02							0.01			
Fe	2.49	2.44	2.56	2.37	2.49	2.81	2.15	2.37	2.86	2.49	2.50	2.80	2.52	2.48	2.46	2.50	2.91
Mg	3.03	3.14	3.12	3.44	3.33	3.05	3.71	3.57	3.21	3.61	3.74	3.44	3.82	3.90	3.94	3.98	3.63
Mn	0.01	0.02	0.03	0.03	0.02		0.05	0.03		0.01	0.03		0.03	0.02		0.02	
Ca	0.05	0.07	0.05	0.04	0.07	0.04	0.06	0.02	0.03		0.02	0.02	0.03			0.02	0.03
Na	0.35	0.30	0.22	0.31	0.16	0.29	0.21	0.16	0.15	0.21	0.13	0.13	0.13		0.13		
	15.28	15.25	15.19	15.29	15.16	15.20	15.18	15.12	15.09	15.12	15.13	15.09	15.12	14.99	15.08	15.01	15.01

SiO_2	53.25	53.57	54.43	54.52	53.69	54.21	55.16	55.29	55.06	55.71
Al_2O_3	4.57	3.97	3.64	2.97	2.79	2.47	1.93	1.57	1.34	0.97
Cr_2O_3	0.27	0.26	0.27	bd	0.22	bd	0.12	bd	bd	bd
TiO_2	bd	0.11	bd	bd	bd	bd	bd	bd	bd	bd
FeO	20.94	20.83	21.87	20.84	20.77	21.55	19.15	21.14	21.52	21.60
MgO	19.33	19.67	19.70	19.37	19.68	19.49	21.45	19.93	20.12	20.42
MnO	bd	0.15	0.21	bd	0.19	bd	0.29	bd	bd	bd
CaO	bd	bd	bd	bd	0.10	bd	0.28	bd	bd	bd
Na_2O	bd	bd	bd	bd	bd	bd	bd	bd	bd	bd
	98.36	98.56	100.12	97.70	97.44	97.72	98.38	97.93	98.04	98.70
Si	7.59	7.63	7.69	7.81	7.74	7.80	7.81	7.91	7.89	7.93
Al	0.77	0.67	0.60	0.50	0.47	0.42	0.32	0.26	0.22	0.16
Cr	0.03	0.03	0.03		0.03		0.01			
Ti		0.01								
Fe	2.50	2.48	2.50	2.50	2.50	2.59	2.27	2.53	2.58	2.57
Mg	4.15	4.17	4.15	4.14	4.23	4.18	4.53	4.25	4.30	4.33
Mn		0.02	0.03		0.02		0.03			
Ca					0.01		0.04			
Na										
	15.04	15.01	15.00	14.95	15.00	14.99	15.01	14.95	14.99	14.99

The orthoamphibole compositions are selected to show the continuous range across much of the gedrite – anthophyllite solid-solution series. All iron is listed as FeO and the mineral formulae are calculated on the basis of 23 oxygens. The analyses were carried out on the energy-dispersive electron microprobe designed and housed in the Department of Earth Sciences, University of Cambridge, using an accelerating voltage of 20 kV, specimen current of 45 nA and count time of 80 seconds with a typical input rate of between 4 and 5 KPPS.

(fig. 4c). Fig. 4a and b come from the same grain being less than 1 mm apart in a direction parallel to the c-axis and show a complete change in type and amount of Al content. Similar patterns may be seen in sections normal to the c-axis. Some crystals contain occasional blebs (30 μm long) of a higher-Al amphibole set in a low-Al matrix (fig. 4a) which appear to be small-scale varieties of the larger banded features. Different grains in the same rock behave differently. Fig. 3b shows traverses for short distances into two different grains (A, C) and one right across a third (B). The early steps in traverses A and C go in markedly different directions, while the 'zoning' in traverse B is distinctly asymmetric. Grain boundaries all have a similar composition, a pattern also seen in other samples. Fig. 3e shows a traverse which crosses a number of grain boundaries, all of which

approximate to an Al content of about 0.9 formula units. A similar pattern has been noted elsewhere by Chinner and Fox (1974). Fig. 3d shows a rapid alternation between anthophyllite-rich and gedrite-rich bands with an absence of points in the range Al 0.5 to 0.7. This is the nearest observational evidence of the type that may be expected for sub-solvus growth of two compositionally distinct orthoamphiboles, in which case the narrow compositional gap would indicate growth near the top of the solvus.

The orthoamphiboles appear to represent extremely uneven growth with local composition changing very fast and erratically both across and along grains. It is difficult to believe that this can be anything other than a growth feature. There is no evidence for the type of growth reported by Spear (1980) in which a distinct gedritic amphibole
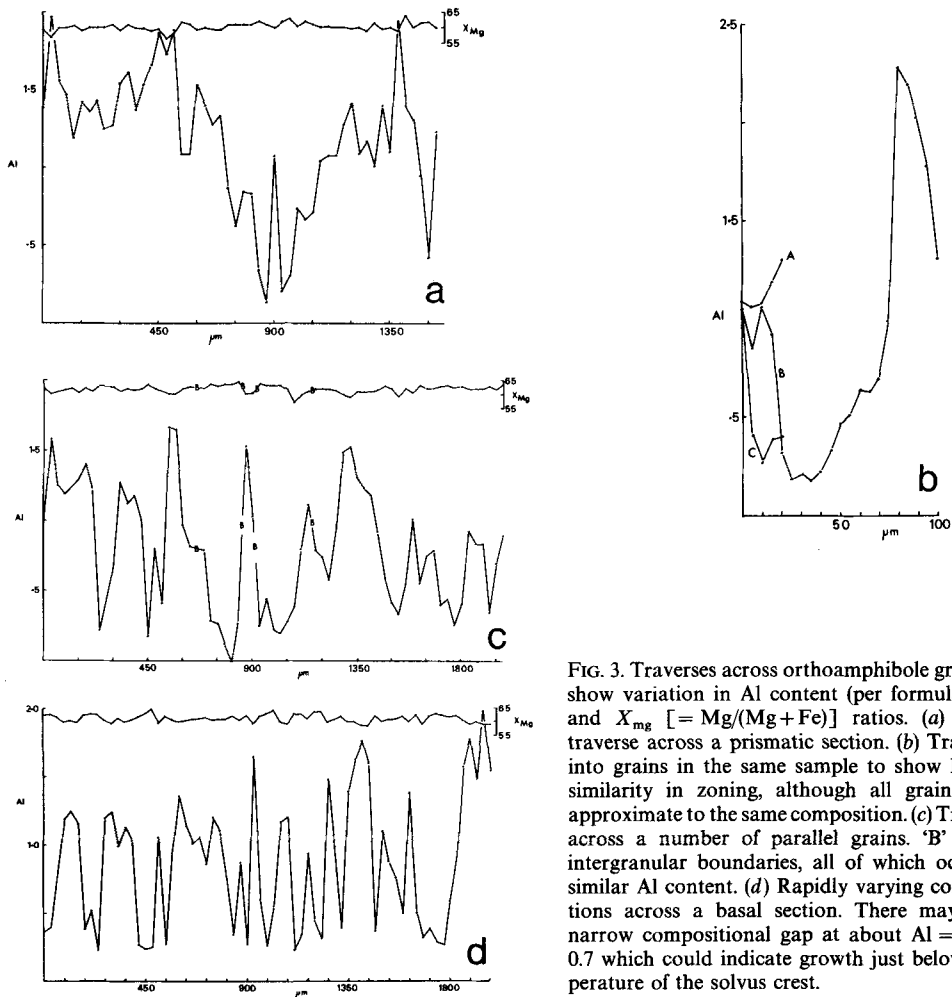
FIG. 3. Traverses across orthoamphibole grains to show variation in Al content (per formula unit) and X_{mg} [$= Mg/(Mg + Fe)$] ratios. (a) Single traverse across a prismatic section. (b) Traverses into grains in the same sample to show lack of similarity in zoning, although all grain edges approximate to the same composition. (c) Traverse across a number of parallel grains. 'B' marks intergranular boundaries, all of which occur at similar Al content. (d) Rapidly varying compositions across a basal section. There may be a narrow compositional gap at about Al = 0.6 to 0.7 which could indicate growth just below temperature of the solvus crest.
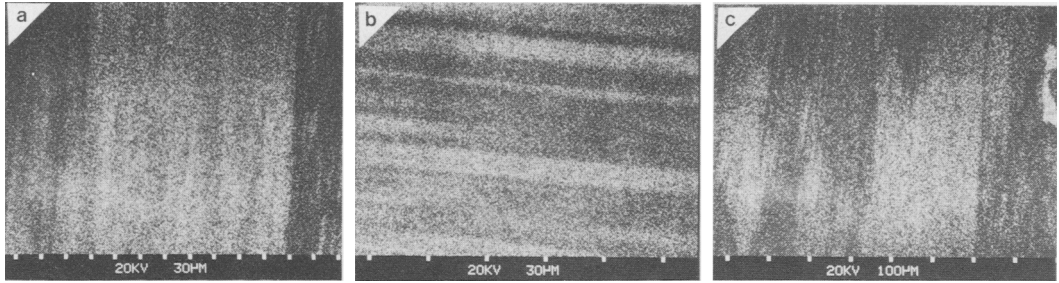
FIG. 4. Al-$K\alpha$ scans along long axes of orthoamphibole grains, showing rapid variation both along and across grains in Al content. The length of the scale bar is indicated in each case.

and a distinct anthophyllitic amphibole are inter-grown with each other. Neither Al-$K\alpha$ X-ray photographs nor electron microscope images show the sort of regular lamellar intergrowth of such distinct phases as noted by Spear (1980, fig. 2C, D), nor is there evidence of coarse bladed intergrowths of compositionally distinct phases (op. cit., fig. 2A).

Exsolution microstructures. Although the compositions of the orthoamphiboles span Spear's proposed solvus there are no exsolution textures visible on a light-optical scale. Thinned specimens were therefore prepared for transmission electron microscopy by ion-beam thinning standard petrographic sections mounted on 3 mm diameter grids. Observations were made at low and high resolutions using a JEM100CX electron microscope. Compositions of observed regions were inferred from the larger-scale electron-probe analyses as microanalysis facilities were not available on the electron microscope used.

Observations on over ten orthoamphibole specimens showed that all had exsolved to some extent. The complex compositional zoning resulted in a range of microstructures associated with exsolution at different temperatures on the limbs of the solvus. In anthophyllitic compositions exsolution is virtually absent compared with gedritic compositions, a feature also noted by Spear (1980) who accounted for it by suggesting that the anthophyllite limb of the solvus was steeper than the gedrite limb. Compositions near the middle of the solvus show regular exsolution lamellae, usually slightly wavy but lying on approximately (010) planes of the orthoamphibole structure. The lamellae are generally less than 1000 Å (0.1 μm) wide (fig. 5a).

Abrupt bulk compositional changes result in lower-temperature exsolution with a decreased nucleation rate. This leads to wider-spaced lamellae and the formation of a solute concentration profile adjacent to them. As the compositions between the
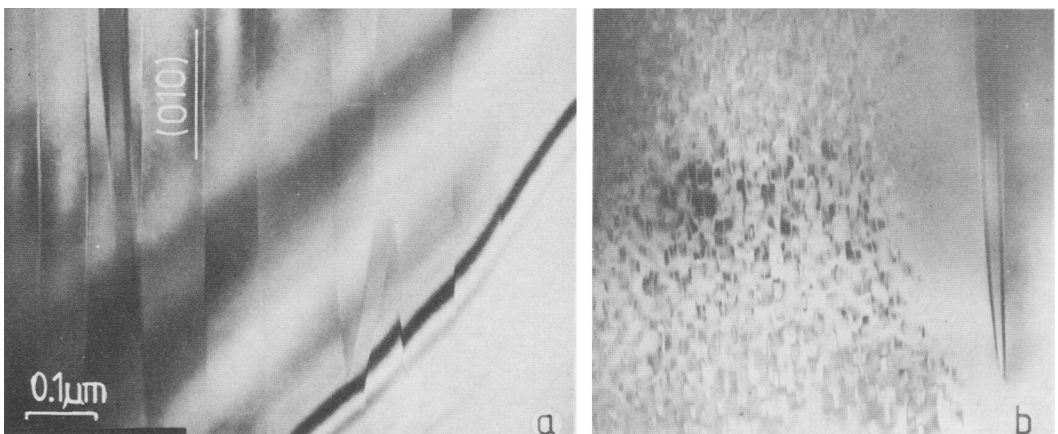

FIG. 5. Exsolution microstructures in the orthoamphibole. (a) Low-magnification transmission electron micrograph of anthophyllite-gedrite lamellae in orthoamphibole of composition near 40% gedrite. (b) A lamella of anthophyllite mantled by a precipitate free zone. A second generation of small (010) precipitates have nucleated between such widely spaced lamellae.
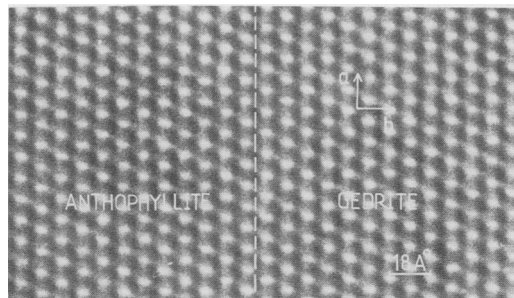
FIG. 6. High resolution c-axis projection electron micrograph of an anthophyllite–gedrite interface. No structural irregularities can be detected.

lamellae become supersaturated on falling temperature, secondary exsolution takes place leading to microstructures such as shown in fig. 5b. Such phenomena are common during silicate exsolution and have been discussed by Putnis and McConnell (1980) and described in orthoamphiboles by Gittos et al. (1976).

The two illustrated microstructures represent the two extreme cases at the centre and the limb of the solvus. In general the frequency of lamellae is dependent on the overall bulk composition although widely-spaced lamellae are not always accompanied by second-generation exsolution, particularly in more anthophyllite-rich bulk compositions.

High-resolution electron microscopy was used to study the interfaces between lamellae. The interpretation of these many-beam images has been discussed by Veblen and Buseck (1979) who equate the white spot in c-axis projection images with the large A-site in the amphibole structure. A feature of this type of image is that virtually no diffraction contrast exists and hence there is very little contrast difference between the gedrite and anthophyllite. The interfaces therefore, obvious in low magnification diffraction contrast images such as fig. 5, can only be seen if there are some structural irregularities associated with them. In this case all the observed interfaces were found to be coherent and hence virtually indistinguishable from the lamellae (fig. 6). Under these circumstances the diffraction pattern shows none of the splitting of spots commonly associated with exsolution. The coherency is a result of the similarity in the lattice parameters of anthophyllite and gedrite. The a and c axes are almost identical, while the b axes differ by only 1 % in the unstrained state (fig. 6).

Within the anthophyllite, linear defects on (010) planes are not uncommon. Such defects have also been mentioned by Gittos et al. (1976) although their nature was not known. At high resolutions in c-axis projection images the defects are seen to be isolated lamellae of triple-chain biopyribole. Chain-width defects and their high resolution images have recently been extensively studied by Veblen (see e.g. Veblen and Buseck, 1979). In fig. 7 a single triple-chain passes through normal double-silicate-chain amphibole structure. In the antho-
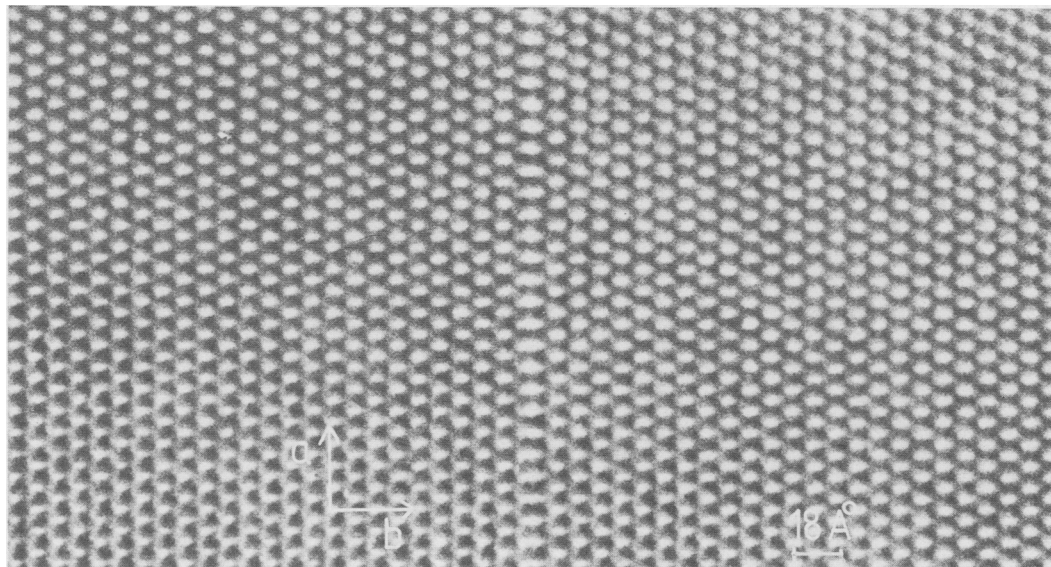

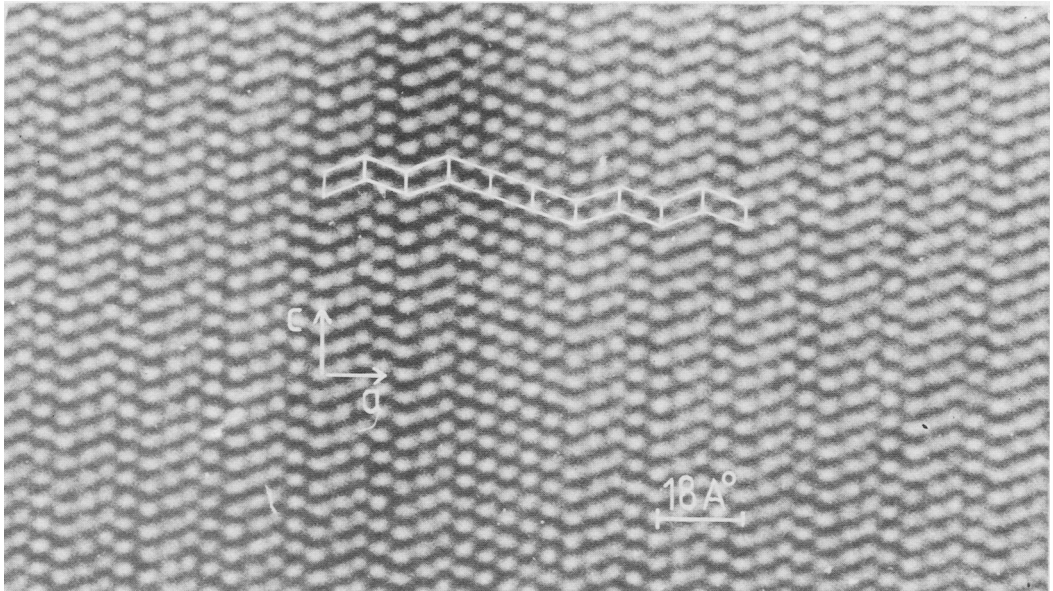FIG. 7. High resolution c-axis projection electron micrograph of a single triple-chain defect in anthophyllite.

FIG. 8. High resolution b-axis projection electron micrograph of a (100) defect in anthophyllite. The defect consists of a 2 unit-cell-thick plate of clinoamphibole.

phyllite studied here such defects rarely exceed two triple-chains in thickness and do not appear to be associated directly with anthophyllite breakdown to layer silicates, a process which is evident in some specimens.

Another common feature of these orthoamphiboles also described by Gittos et al. (1976) is the existence of narrow platelets on (100) which often act as sites for second-generation exsolution. High-resolution electron microscopy reveals these to be strips of clinoamphibole within the orthorhombic matrix. Fig. 8 is a b-axis projection of the structure showing the unit-cell twinning which relates the clino- and ortho- unit cells, and the fault which introduces an extra plate of clinoamphibole 2 unit cells thick. Such faults have been widely discussed in the literature (see e.g. Kirby, 1976) and are attributed to deformation.

Discussion. The solvus in the orthoamphibole system with a steeper anthophyllite than gedrite limb has been qualitatively defined by Spear (1980, fig. 14) as having a crest at about $600 \pm 25 \,°C$. The exsolution microstructures indicate that the Outokumpu orthoamphiboles have exsolved below the solvus temperature. Although the metastable growth of solid solutions below the solvus is not unknown, particularly when growth rates are rapid, it seems more plausible to suggest a growth at temperatures above the solvus for those specimens observed here. The possible growth of two distinct amphiboles separated by a small composi-

tional gap in the solid solution (fig. 3d) could indicate that the effective temperature of growth was just below that of the solvus crest. This possibility is not inconsistent with estimated metamorphic temperatures of about $600 \,°C$ (Treloar et al., 1981).

The erratic compositional variations within the amphiboles which are, after all, occurring in association with what appears to be an equilibrium assemblage composed of phases of limited compositional range is intriguing. It is not unlikely that the large bladed orthoamphibole crystals grew very fast, certainly with little time for the flattening out of marked chemical potential gradients. It is possible to view the variations as resulting either from the rapid overgrowing of original sedimentary variations in the rock chemistry or from the external buffering of one or more compositional parameters.

The assemblages concerned are all polymineralic low variance ones. The constancy of K_D^{Fe-Mg} values between all phases both within and between individual specimens is indicative of an approach to equilibrium. Fe and Mg in the orthoamphiboles show constant ratios within crystals, constant K_D^{Fe-Mg} ratios with the associated phases and no systematic variation with varying Al content in the orthoamphiboles (fig. 3a, c, d). In addition there is a sufficiency of phases present within each rock to form a limiting assemblage capable of buffering the Al content of the orthoamphiboles.

In the event that Al is internally defined the role of Na and the nature of the solid solution series appear to be significant. If the tschermakitic and edenitic substitutions are systematically related with a direct linkage through some mechanism such as charge balancing, it becomes possible to relate the composition of a grain within the gedrite-anthophyllite system to the extent of edenitic substitution and hence, quite simply, to the availability of Na. In the present samples the edenitic substitution is faithfully followed (fig. 2), and it does appear that where Na enters into the amphibole structure all substitutions proceed as theoretically predicted. There is no reason why the orthoamphiboles should not respond to Na availability by taking it into the lattice. There is very little difference in the lattice parameters of gedrite and anthophyllite (fig. 6a) and therefore no spatial restriction on the growth of different solid-solution compositions within the same orthoamphibole grain. Similarly at temperatures of growth near to those of the solvus crest, as in the present case, there will be little change in free energy of the phase over a large part of the solid-solution series. As a result no particular composition will be strongly favoured and a wide variety of solid solution compositions may occur, each of them locally defined by the availability of Na.

In the eventuality that there is no energetic constraint on the amount of substitution that can take place and that lattice parameters are not going to prevent the growth of a phase of varying composition the outstanding problem is what controls the availability of the Na which is so readily accepted by the orthoamphibole. There are two distinct possibilities: one is that the amphiboles are overgrowing relict variations in Na content that predate the metamorphism; and the other that μ_{Na} may be variably externally controlled, so that Na is available in the rocks through the medium of the fluid phase in quantities varying rapidly both spatially and temporally, with the result that varying amounts of Na are available to different parts of the rock. Both possibilities imply that the amphiboles grow sufficiently fast for compositional variations to be frozen before they can re-equilibrate through diffusion with a new growth and that at any stage the amphibole is in equilibrium with the rest of the rock. There is support for the second possibility in the way that orthoamphibole boundaries tend to a constant composition, which would follow from the final equilibration of the assemblage with the fluid phase, but might not be expected if the amphibole's chemistry is the result of overgrowing relict compositional irregularities.

REFERENCES

Campbell, D. S. (1980) *Trans. R. Soc. Edinburgh,* **71,** 185–200.

Chinner, G. A., and Fox, J. S. (1974) *Geol. Mag.* **111,** 397–408.

Eskola, P. (1933) *Bull. Comm. Geol. Finland,* **103,** 26–44.

Gaal, G., Koistinen, T., and Mattila, E. (1975) *Bull. Geol. Surv. Finland,* **271,** 1–67.

Gittos, M. R., Lorimer, G. W., and Champness, P. E. (1976) In *Electron Microscopy in Mineralogy,* Wenk, H. R. *et al.* (eds.), Springer-Verlag, Berlin, 238–47.

Huhma, A., and Huhma, M. (1970) *Bull. Geol. Soc. Finland,* **42,** 57–88.

James, R. S., Grieve, R. A. F., and Pauk, L. (1978) *Am. J. Sci.* **278,** 41–63.

Kirby, S. H. (1976) In *Electron Microscopy in Mineralogy,* Wenk, H. R. *et al.* (eds.), Springer-Verlag, Berlin, 465–72.

Koistinen, T. J. (1981) *Trans. R. Soc. Edinburgh,* **72,** 115–58.

Makela, M. (1974) *Bull. Geol. Surv. Finland,* **267,** 1–45.

Mikkola, A. (1980) Ibid. **305,** 1–22.

Peltola, E. (1978) *Econ. Geol.* **73,** 461–77.

Putnis, A., and McConnell, J. D. C. (1980) *Principles of Mineral Behaviour,* Blackwells, Oxford.

Robinson, P., and Jaffe, H. W. (1969) *Mineral. Soc. Am. Spec. Paper,* **2,** 251–74.

——Ross, M., and Jaffe, H. W. (1971) *Am. Mineral.* **56,** 1005–41.

Ross, M., Papike, J. J., and Shaw, K. W. (1969) *Mineral. Soc. Am. Spec. Paper,* **2,** 275–99.

Spear, F. S. (1980) *Am. Mineral.* **65,** 1103–18.

Stoddard, E. F. (1979) Geol. Soc. Am. Abs. with Progs., Cordilleran Section 11, 130.

Treloar, P. J., Koistinen, T. J., and Bowes, D. R. (1981) *Trans. R. Soc. Edinburgh,* **72,** 201–15.

Tuominen, H. V., and Mikkola, T. (1950) *Bull. Comm. Geol. Finland,* **150,** 67–92.

Vallance, T. G. (1967) *J. Petrol.* **8,** 84–96.

Veblen, D. R., and Buseck, P. R. (1979) *Am. Mineral.* **64,** 687–700.